

Overexpression of claudin-7 decreases the paracellular Cl^- conductance and increases the paracellular Na^+ conductance in LLC-PK1 cells

Michele D. Alexandre, Qun Lu and Yan-Hua Chen*

Department of Anatomy and Cell Biology, East Carolina University, Brody School of Medicine, Greenville, NC 27858, USA

*Author for correspondence (e-mail: chen@mail.ecu.edu)

Accepted 23 March 2005

Journal of Cell Science 118, 2683-2693 Published by The Company of Biologists 2005
doi:10.1242/jcs.02406

Summary

Tight junctions form the primary barrier regulating the diffusion of fluid, electrolytes and macromolecules through the paracellular pathway. Claudins are the major structural and functional components of tight junction strands and are considered as the best candidates for forming paracellular channels. They are a family of integral membrane proteins with more than 20 members and show distinct tissue distribution patterns. In this study, we found that claudin-7 is expressed in the distal and collecting tubules and the thick ascending limb of Henle of porcine and rat kidneys. To investigate the role of claudin-7 in paracellular transport, we have overexpressed a mouse *claudin-7* construct in LLC-PK1 cells. Overexpression of claudin-7 did not affect the expression and localization of endogenous claudin-1, -3, -4, -7, and ZO-1. However, transepithelial electrical resistance in claudin-7-overexpressing cells was greatly increased. In addition, electrophysiological measurements revealed a dramatic reduction of dilution potentials in claudin-7-overexpressing cells compared to that of control cells. To determine which ions are responsible for the effects of claudin-7

overexpression on transepithelial electrical resistance and dilution potentials, we applied an ion substitution strategy. When NaCl was replaced with sodium aspartate, transepithelial electrical resistance was significantly decreased and dilution potentials were increased in claudin-7-overexpressing cells as compared to controls, the opposite effects from that of using NaCl. Furthermore, when NaCl was substituted by arginine-HCl or lysine-HCl, the increase in transepithelial electrical resistance was greater and the reduction in dilution potentials was smaller. Taken together, our studies demonstrated for the first time that the effect of claudin-7 overexpression in LLC-PK1 cells on paracellular transport is mediated through a concurrent decrease in the paracellular conductance to Cl^- and an increase in the paracellular conductance to Na^+ . These results support the model that claudin-7 may form a paracellular barrier to Cl^- while acting as a paracellular channel to Na^+ .

Key words: Claudin-7, Tight junction, Transepithelial electrical resistance, Dilution potential, Paracellular flux, LLC-PK1 cells

Introduction

Multicellular organisms contain distinct fluid compartments that are established by epithelial cells. In order to maintain tissue homeostasis, the space between adjacent cells has to be sealed to prevent the free diffusion of substances. This intercellular space is called the paracellular pathway, and the tight junction is the structure that maintains this seal (Wong and Goodenough, 1999; Tsukita and Furuse, 2000; Mitic et al., 2000; Gonzalez-Mariscal et al., 2003; Schneeberger and Lynch, 2004). The tight junction functions as a gatekeeper of the paracellular pathway, regulating the passage of ions, solutes, and immune cells through the spaces between epithelial cells. The recent identification of tight junction proteins, namely the claudin family, has prompted the investigation of the molecular structure and mechanisms underlying the paracellular transport.

Claudins are a family of tetraspan transmembrane proteins with molecular masses of ~23 kDa and have been identified as major structural and functional components of tight junction strands (Furuse et al., 1998; Morita et al., 1999; Heiskala et al.,

2001). Claudins have specific tissue distribution patterns. It has been reported that, among its more than twenty members, at least eleven claudins (claudin-1, -2, -3, -4, -7, -8, -10, -11, -14, -15 and -16) are expressed in the different segments of renal tubules (Kiuchi-Saishin et al., 2002; Reyes et al., 2002; Li et al., 2004). Interestingly, claudin-7 and -8 have similar distribution patterns, with both being present in the distal and collecting tubules of the kidney (Li et al., 2004). Recently, there have been several important studies indicating that claudins form unique paracellular channels responsible for the paracellular ion permeability (Turksen and Troy, 2002; Tang and Goodenough, 2003; Anderson et al., 2004; Li et al., 2004). The first evidence to show the influence of a claudin on paracellular ion selectivity is from the work by Van Itallie et al. (Van Itallie et al., 2001). In this study, they showed that the overexpression of claudin-4 in MDCK II cells decreased the paracellular conductance through a selective decrease in Na^+ permeability without a significant effect on Cl^- permeability. Furthermore, Colegio et al. (Colegio et al., 2003) from the same laboratory reported that substituting a negative for a

positive charge in the first extracellular domain of claudin-4 increased the paracellular Na^+ permeability. Substituting positive for negative charges in the first extracellular domain of claudin-15 also changed the paracellular charge selectivity from Na^+ to Cl^- . Other studies have shown that claudin-2 formed cation-selective channels in MDCK cells, and its expression in high-resistance MDCK I cells lacking claudin-2 caused >20-fold decrease in transepithelial electrical resistance (TER) (Furuse et al., 2001; Amasheh et al., 2002).

To examine whether the cell background influences the electrophysiological properties of individual claudins, Van Itallie et al. (Van Itallie et al., 2003) introduced claudin-2, -4, -11 and -15 into both cation-selective MDCK II cells and anion-selective LLC-PK1 cells. Expression of claudin-4 and -11 in MDCK II cells decreased the paracellular Na^+ permeability, whereas claudin-2 and -15 had no effect in this cell line. Expression of claudin-2 and -15 in LLC-PK1 cells increased the paracellular Na^+ permeability, whereas claudin-4 and -11 did not show any effect. These results indicate that the role of each claudin in paracellular transport can be more easily detected when it has the opposite charge selectivity than that of the cell monolayer. For example, claudin-4 reduces the paracellular Na^+ permeability while MDCK II cells are more permeable to cations than anions. Therefore, the role of claudin-4 is more easily detected in MDCK II cells because it has the opposite charge selectivity than that of MDCK II cells. Although the expression of claudin-8 in MDCK II cells has been shown recently to reduce the paracellular conductance and Na^+ permeability (Jeansonne et al., 2003; Yu et al., 2003), the role of claudin-7 in paracellular transport is unknown. In this study, we found that claudin-7 was localized in the distal and collecting tubules as well as the thick ascending limb of Henle (TALH) of porcine and rat kidneys. Overexpression of claudin-7 in cultured LLC-PK1 cells resulted in a significant increase in TER and a dramatic reduction in dilution potentials. Using an ion substitution method, we demonstrated that these effects were due to a decrease in the paracellular conductance to Cl^- and an increase in the paracellular conductance to Na^+ , concurrently. Our results suggest that claudin-7 may form a paracellular barrier to Cl^- while acting as a paracellular channel to Na^+ .

Materials and Methods

Antibodies and reagents

The rabbit polyclonal anti-claudin-1, -2, -3, -4, -7, and anti-ZO-1 antibodies were purchased from Zymed (South San Francisco, CA, USA). The rabbit anti-GFP polyclonal antibody was obtained from MBL (Medical and Biological Laboratories Co. Ltd., Japan). The mouse monoclonal anti-actin antibody was from Calbiochem (San Diego, CA, USA). The Cyt3-conjugated anti-rabbit and anti-mouse IgG were obtained from Jackson ImmunoResearch (West Grove, PA, USA). FITC-conjugated goat anti-rabbit IgG and HRP-conjugated anti-rabbit and anti-mouse secondary antibodies were purchased from Roche Applied Sciences (Indianapolis, IN, USA) and Promega (Madison, WI, USA), respectively. Radio-labeled [^3H]mannitol was from MP Biochemicals Inc. (Irvine, CA, USA). All chemicals and reagents were from Sigma, unless indicated otherwise; all tissue culture reagents were purchased from Invitrogen (Carlsbad, CA, USA). Transwell and Snapwell (pore size, 0.4 μm) were from Corning Costar (Cambridge, MA, USA).

Generation of the *claudin-7* construct

The full-length *claudin-7* cDNA was obtained from mouse kidney total RNA isolated by guanidinium thiocyanate-phenol-chloroform extraction (Jeansonne et al., 2003). Briefly, random decamers were used as a first-strand primer to synthesize the first-strand DNA sequence from the total RNA (Ambion Inc, Austin, TX, USA). Twenty-one bp from the N terminus of claudin-7 and 22 bp from the C terminus of claudin-7 were used as specific PCR primers (Morita et al., 1999) to yield the full-length *claudin-7* cDNA. The RT-PCR products were directly subcloned into the TOPO vector (Invitrogen, Carlsbad, CA), and the *claudin-7* sequence was verified by DNA sequencing. To generate the *claudin-7*-GFP construct, *claudin-7* cDNA was released from the TOPO vector and subcloned into the mammalian expression vector pEGFP (Clontech Laboratories) with the GFP tagged at the C terminus of claudin-7.

Cell culture and transfection

LLC-PK1 cells (a porcine kidney epithelial cell line, kindly provided by J. A. Marrs, Indiana University Medical Center, IN, USA) were grown in DMEM/F12 medium containing 10% FBS, 100 units/ml of penicillin, and 100 $\mu\text{g}/\text{ml}$ streptomycin in a humidified air–5% CO_2 atmosphere at 37°C. *claudin-7*-GFP and empty GFP vectors were transfected into LLC-PK1 cells using the Lipofectamine 2000 Reagent (Invitrogen, Carlsbad, CA, USA). After 48 hours incubation, transfected cells were transferred from 6-well plates to 100-mm plates, and geneticin (G418) was added to the plates the next day. Following the geneticin selection, GFP-positive cells (mixed clones) were selected again by using a high speed Flow Cytometry Instrument (Becton Dickinson, Flow Cytometry-Confocal Microscopy Core Facility at East Carolina University Brody School of Medicine). This method allowed us to obtain 100% claudin-7-GFP-positive cells, and therefore, detect the effect of claudin-7 on the paracellular transport more easily. We also used the limited dilution method to obtain the individual clones (Jeansonne et al., 2003) and a total of twelve clones were selected. Transfected cells were cultured in DMEM/F12 containing 500 $\mu\text{g}/\text{ml}$ geneticin to maintain the selection pressure.

Immunofluorescence and confocal microscopy

Fresh porcine kidneys were obtained from a local slaughterhouse. Adult rats were purchased from Harlan (Indianapolis, IN, USA). Cubes of tissue were cut 0.5 cm from the kidney cortex of both pig and rat and immediately immersed in 2-methylbutane on dry ice before transferring to liquid nitrogen. Eight-micrometer frozen sections were cut using a cryostat. For the immunofluorescent staining, sections were fixed in 100% methanol for 8 minutes at –20°C and washed with PBS for 5 minutes before incubating with 0.2% Triton X-100 for 10 minutes at room temperature. Sections were incubated in 100 mM glycine for 15 minutes to quench the autofluorescence and then blocked in 5% normal goat serum for 30 minutes at 37°C. BSC-1 (Na/K/2Cl cotransporter), TSC (Na/Cl cotransporter; anti-BSC-1 and TSC antibodies were generous gifts from Mark Knepper, NIH), and NCX1 (Na⁺/Ca²⁺ exchanger; Novus, CO, USA) were used as specific markers for the TALH, distal tubules and collecting tubules, respectively. Both BSC-1 and TSC were rabbit polyclonal antibodies (pAb) while NCX1 was a mouse monoclonal antibody (mAb). The dilution was 1:100 for anti-claudin-7 antibody or 1:50 for BSC-1, TSC and NCX1 antibodies.

LLC-PK1 cells grown on glass coverslips were fixed with 100% methanol at –20°C for 5 minutes. Cells were blocked with 5% BSA for 60 minutes at room temperature and incubated with primary antibodies against claudin-1, -2, -3, -4, -7, and ZO-1 at 1:100 dilution. All antibodies were diluted in PBS containing 5% BSA. After washing, cells were incubated with Cyt3-conjugated anti-rabbit secondary antibody (1:600) for 60 minutes at room temperature. For the specific peptide inhibition procedure, anti-claudin-2 antibody

(1:100 dilution) was incubated with 100 µg/ml of claudin-2 peptide (Zymed) for 30 minutes at room temperature before applying the antibody to the LLC-PK1 cells. Coverslips were mounted with ProLong Antifade Kit (Molecular Probes Inc., OR, USA). Samples were analyzed and photographed using a Zeiss Axiovert S100 or Zeiss LSM 510 laser confocal scanning microscopy (Carl Zeiss Inc., Thornwood, NY, USA).

Western blotting

LLC-PK1 parental cells and cells stably transfected with the GFP vector alone or the *claudin-7*-GFP construct were washed three times in PBS and then lysed in RIPA buffer (1% Triton X-100, 0.5% sodium deoxycholate, 0.2% SDS, 150 mM NaCl, 10 mM Hepes, pH 7.3, 2 mM EDTA, 10 µg/ml each of chymostatin, leupeptin and pepstatin A). After 20 minutes incubation at 4°C, lysates were homogenized on ice by passing 20 times through a 22-gauge needle and centrifuged at 15,000 *g* for 30 minutes at 4°C. The total protein concentration of each sample was measured using the BCA protein assay kit (Pierce, Rockford, IL, USA) and adjusted to equal concentration (1 mg/ml).

The cell lysates in the SDS sample buffer were separated by SDS-PAGE and transferred to nitrocellulose membranes. The membrane was then blocked in 5% non-fat dried milk in PBS plus 0.1% Tween 20 and incubated with primary antibodies for 1.5 hours followed by incubation with appropriate secondary antibodies for 1 hour. Dilutions for the primary antibodies were as follows: anti-claudin-1, -2, -3, -4, -7, 1:1000; anti-ZO-1, 1:2000; anti-actin, 1:5000. The dilutions used for HRP-conjugated anti-rabbit and anti-mouse secondary antibodies were 1:2500. After blotting, the signals were detected by enhanced chemiluminescence (Amersham, Arlington Heights, IL, USA) on X-OMAT film. The western blots were quantified using a DuoScan (AGFA Corp, NY, USA) densitometer and analyzed by the Imaging J System (NIH, MD).

Measurement of transepithelial electrical resistance (TER)

For TER measurements, LLC-PK1 cells stably transfected with *claudin-7*-GFP or vector alone were plated on Transwell membranes at the density of 2×10^5 cells/cm². A Millicell-ERS voltohmmeter (Millipore Corp., Bedford, MA, USA) was used to determine the TER value (Chen et al., 2002). TER measurements were performed in culture medium or in P buffer containing 140 mM NaCl, 2 mM CaCl₂, 1 mM MgCl₂, 10 mM glucose, 10 mM Hepes, pH 7.3. To examine the effect of Na⁺ and Cl⁻ on TER separately, some of the TER measurements were performed in the modified P buffer with 140 mM NaCl replaced by 140 mM arginine-HCl, or 140 mM lysine-HCl, or 140 mM sodium aspartate. At neutral pH, arginine and lysine are positively charged while aspartate is negatively charged in the solution. HCl dissociates into H⁺ and Cl⁻ in the solution, and H⁺ will combine with OH⁻ to form water at pH 7.3.

All TER values were calculated by subtracting the resistance measured in the blank insert from the resistance measured in the insert with the monolayer and then multiplied by the surface area of the membrane.

Electrophysiological measurements

For electrophysiological measurements, control and claudin-7-overexpressing cells were grown on Snapwell filters. After the monolayer reached confluence, the filter ring containing the cell monolayer was detached and mounted on a slider that can be inserted into the EasyMount chamber (Warner Instruments Inc., Hamden, CT). The chambers were filled with one of the following buffers: P1, 140 mM NaCl; P2, 70 mM NaCl, 140 mM mannitol; P3, 35 mM NaCl, 210 mM mannitol. Mannitol was added to the P2 and P3 solutions in order to maintain the same osmolarity condition as P1. In some

experiments, NaCl in P1, P2 and P3 was replaced by arginine-HCl or lysine-HCl to determine the effect of Cl⁻ without Na⁺ or replaced by sodium aspartate to eliminate the effect of Cl⁻. All of the above buffers contained 2 mM CaCl₂, 1 mM MgCl₂, 10 mM Hepes, 10 mM glucose, pH 7.3. During the experiment, the buffer was maintained at 37°C and bubbled constantly with 95% air-5% CO₂.

Each electrode set consisted of two pairs of Ag/AgCl electrodes, one for passing current and the other for sensing voltage. The electrode was inserted into a pipette tip and connected to the buffer in the chamber via a 3 M KCl agar bridge. Voltage and current signals were sent to the VCC MC6 Voltage/Current Clamp instrument through DM MC6 input modules (Warner Instruments Inc., Hamden, CT, USA). The asymmetry voltage between the electrodes and the liquid junction potentials were compensated by an offset system built inside the instrument before measuring the dilution potentials. The dilution potential is defined as $V_{dp} = V_2 - V_1$, where V_2 is the apical voltage and V_1 is the basal voltage. When both apical and basal chambers contained the same P1 buffer, no dilution potential was generated. After replacing P1 with P2 or P3 buffer in the basal chamber, a dilution potential was produced because of the concentration gradient and charge selectivity of the monolayer. We choose to change the buffer in the basal chamber because it apparently disturbed the integrity of the monolayer least (Yu et al., 2003). All dilution potential values were obtained after subtracting the value measured in the blank insert.

Paracellular flux measurements

Urea

For the measurement of the paracellular urea flux, the basal solution was 120 mM NaCl, 50 mM urea, 2 mM CaCl₂, 1 mM MgCl₂, 10 mM glucose and 10 mM Hepes, pH 7.3. The apical solution was 120 mM NaCl, 50 mM mannitol, 2 mM CaCl₂, 1 mM MgCl₂, 10 mM glucose and 10 mM Hepes, pH 7.3. After one hour of incubation at 37°C, the apical solution was removed, and the urea concentration was measured by an ACE clinical chemistry analyzer (ECU Diagnostic Center). TER was monitored before and after each experiment to confirm that the monolayer remained intact during flux experiments.

Mannitol

Paracellular tracer flux experiments using [³H]mannitol were performed according to the method of McCarthy et al. (McCarthy et al., 2000) with some modifications. Monolayers transfected with vector alone or *claudin-7*-GFP were grown on Transwell membranes. Fresh culture medium supplemented with 1 mM mannitol was added to both apical and basal chambers. In addition, the apical medium contained 1 µCi/ml of [³H]mannitol. The monolayers were incubated at 37°C to allow apical to basolateral diffusion of the tracer. After 1 hour of incubation, a 100 µl sample was removed from the basal chamber, and 100 µl of fresh medium with 1 mM unlabeled mannitol was then added. The 100 µl samples were added to 4 ml UniScint BD (National Diagnostics, Atlanta, GA, USA), and the radioactivity was determined in a Tri-Carb liquid-scintillation Analyzer (Packard Instrument Co., Meriden, CT, USA).

Statistical analysis

Statistical analysis was performed using either Origin50 (OriginLab, MA, USA) or Sigmaplot (Systat Software, Inc. CA, USA) softwares. The differences between two groups were analyzed using the unpaired Student's *t*-test. Two-way ANOVA was performed if comparisons involved more than two groups. A *P*-value of <0.05 was considered significant.

Results

Localization of claudin-7 in the porcine and rat kidney cortex

We first examined the localization of claudin-7 in the porcine kidney since LLC-PK1 is an epithelial cell line derived from this tissue. Fig. 1A shows the distribution pattern of claudin-7 in the porcine kidney cortex. Claudin-7 was clearly localized at the apical cell junctions in the distal tubule as identified by TSC antibody (Fig. 1Aa,c). Images a and c were taken from adjacent sections since both anti-claudin-7 and TSC were rabbit polyclonal antibodies. The double immunostaining of claudin-7 and NCX1 showed that claudin-7 was also present in the apical cell junctions of collecting tubules (Fig. 1Ae,f). Localization of claudin-7 in these two segments of porcine nephron was similar to those found in the mouse kidney (Alexandre and Chen, 2003; Li et al., 2004). In addition, claudin-7 signal was observed in the thick ascending limb of Henle (TALH) as a punctate staining pattern, which has not been reported previously (see asterisks and arrow in Fig. 1Ag,i). Here the adjacent sections were again used since both anti-claudin-7 and BSC-1 were rabbit polyclonal antibodies. In order to determine whether the signal seen in TALH was porcine kidney-specific, frozen sections of rat kidney cortex

were used to compare the staining pattern of claudin-7 with porcine kidney. As shown in Fig. 1B, claudin-7 was clearly localized at the apical surfaces of the distal and collecting tubules (Fig. 1Ba,e). Claudin-7 signal was also present in the TALH of the rat kidney (Fig. 1Bg), a pattern similar to that seen in porcine kidney. In addition to the apical staining there was strong basal staining for claudin-7, as reported by others (Li et al., 2004). The significance of this basal staining is currently unclear.

Overexpression of claudin-7-GFP did not affect the expression and localization of endogenous claudin-1, -3, -4, -7, and ZO-1

LLC-PK1 is an anion-selective cell line that expresses at least five claudin members, as shown in Fig. 2A. As indicated in Fig. 2A, claudin-1 (a), -3 (c), -4 (d) and -7 (e) were clearly localized at the cell-cell contact area. However, the immunostaining signal for claudin-2 was prominently localized to the cell nucleus (Fig. 2A,b). There is very little cell junctional staining of claudin-2. This claudin-2 antibody recognized the porcine species since frozen sections of porcine kidney showed strong tubular staining when using this antibody (Fig. 2A, insert in b). To investigate the role of claudin-7 in paracellular transport,

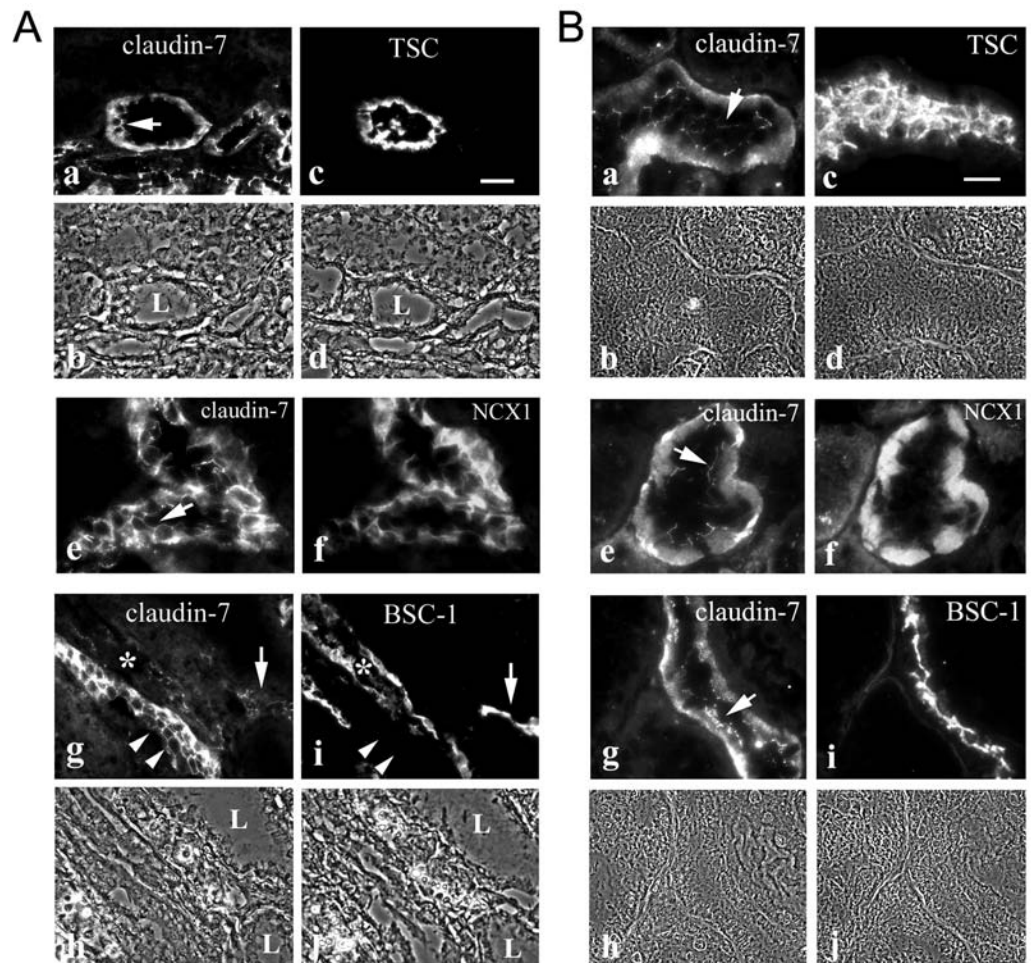


Fig. 1. Localization of claudin-7 in porcine (A) and rat (B) kidney cortex. Frozen sections of kidney cortex were immunostained with anti-claudin-7 antibody and tubular markers Claudin-7 was found to be localized in epithelial cells of the distal and collecting tubules using the distal tubular marker TSC (a and c) and the collecting tubular marker NCX1 (e and f). Because all the antibodies used were rabbit polyclonal antibodies the images in a and c, and in g and i are from adjacent sections (b and d, and h and j are the corresponding phase-contrast images). Images in e and f are from the same section with double immunolabeling. (A) In porcine kidney, claudin-7 is present in the apical cell junctions (arrows in a and e). Claudin-7 was also present in a punctate pattern at the thick ascending limb of Henle (TALH), identified by BSC-1 (asterisks and arrows in g and i). The junctional staining of claudin-7 (indicated by two arrowheads in g) was not in the TALH as it was not co-localized with the BSC-1 staining (two arrowheads in i). L: lumen of the tubule. (B) In rat kidney, Claudin-7 was present in the distal tubule (a), collecting tubule (e) and TALH (g). Arrows in a, e, and g indicated the claudin-7 signal at the apical surface of tubules. Scale bar: 30 μ m (A) and 20 μ m (B).

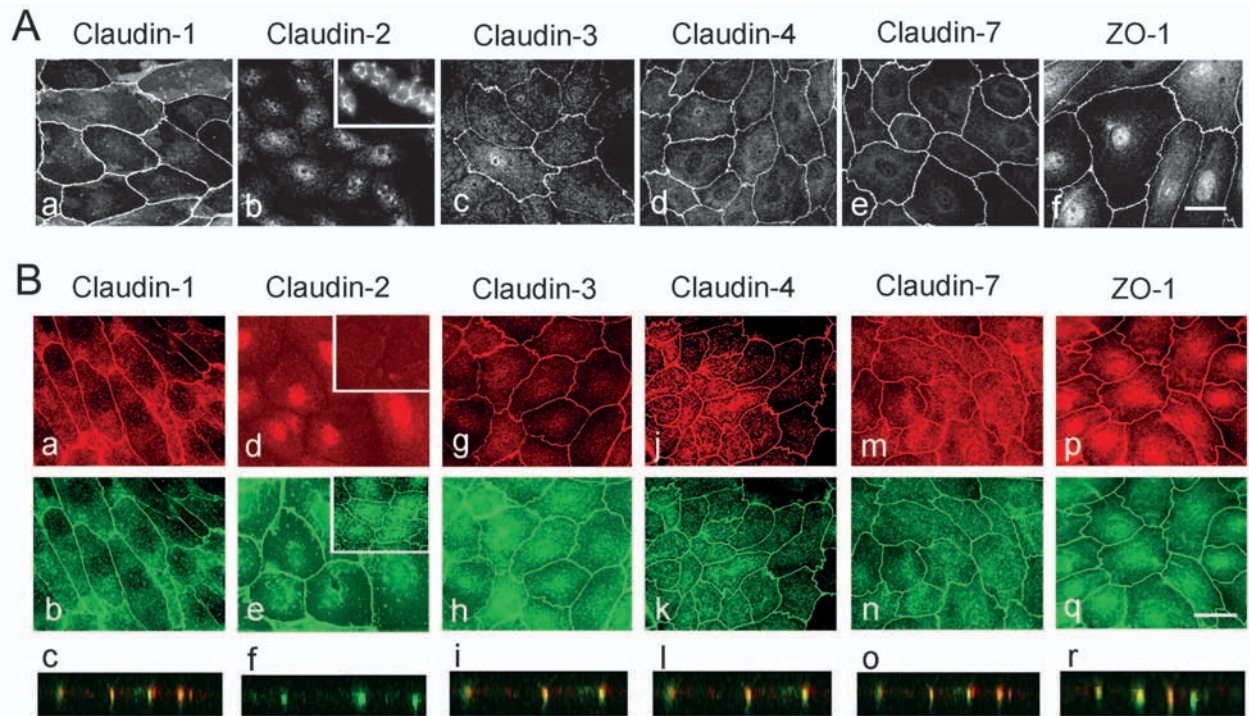


Fig. 2. Expression of claudin-7-GFP did not affect localization of endogenous tight junction proteins. LLC-PK1 cells with or without transfection were grown on coverslips and then fixed in 100% methanol. (A) Localization of tight junction proteins in parental LLC-PK1 cells. Immunostainings for claudin-1 (a), -3 (c), -4 (d), -7 (e) and ZO-1 (f) were clearly present at the cell-cell junction while claudin-2 signal (b) was predominantly localized in the nucleus. This claudin-2 antibody readily recognized the porcine species as seen in the tubular staining of the frozen section of porcine kidney (insert in b). (B) Localization of endogenous tight junction proteins in LLC-PK1 cells expressing claudin-7-GFP. Cells were double-labeled with GFP (b,e,h,k,n,q) and anti-claudin antibodies (a,d,g,j,m,p). Claudin-7-GFP was closely co-localized with claudin-1, -3, -4, -7 and ZO-1, but not claudin-2, at the cell-cell junction area. The staining of the nucleus (d) was claudin-2-specific since this signal was completely abolished after pre-incubation of claudin-2 antibody with claudin-2 peptide prior to the antibody staining procedure (insert in d). This preabsorption/specific peptide inhibition step did not affect the GFP signal of claudin-7-GFP (insert in e). Confocal x-z images (c,f,i,l,o,r) were the superimposed images of claudin-1, -2, -3, -4, -7 and ZO-1 with claudin-7-GFP. Co-localization of tight junction proteins and claudin-7-GFP is seen in yellow. Bar: 15 μ m.

we introduced claudin-7 tagged with GFP to LLC-PK1 cells. Overexpression of claudin-7-GFP did not affect the localization of endogenous claudin-1, -2, -3, -4, -7, and ZO-1 as shown in Fig. 2B. The exogenous claudin-7 labeled by GFP (Fig. 2Bb,e,h,k,n,q) was well co-localized with immunostaining signals for claudin-1 (a), -3 (g), -4 (j), -7 (m), and ZO-1 (p). Anti-claudin-2 signal (Fig. 2Bd) was mainly localized to the cell nucleus, a pattern similar to that of the parental cells (Fig. 2Ab). This nuclear staining was claudin-2-specific since the signal was completely abolished after incubation of claudin-2 antibody with claudin-2 peptide prior to the staining procedure (Fig. 2B, insert in d). The claudin-7-GFP signal was unaffected by this antibody/peptide treatment (Fig. 2B, insert in e). Confocal fluorescence microscopy revealed the Z-axis co-immunolocalization of exogenous claudin-7-GFP with endogenous claudin-1 (c), -3 (i), -4 (l), -7 (o), and ZO-1 (r), whereas claudin-2 signal was absent from the apical tight junction area (f). We have also examined the expression of claudin-8 and -16 in the LLC-PK1 cells with or without the *claudin-7*-GFP transfection. Both of these claudins were not expressed in parental or *claudin-7*-GFP-transfected cells (data not shown).

The expression levels of claudin-1, -2, -3, -4, -7, and ZO-1 were compared in parental, GFP-transfected, and *claudin-7*-

GFP-transfected cells (mixed clones) (Fig. 3). Claudin-2 expression level was decreased in both GFP and claudin-7-GFP-expressing cells compared to that of parental cells (Fig. 3A). Claudin-3 and -4 expression levels were slightly increased in *claudin-7*-GFP-transfected cells compared to those of parental and GFP-transfected cells. The expression levels for claudin-1, -7 and ZO-1 remained the same for all three cell lines. Fig. 3B showed the quantitative analysis of the relative band intensity from three independent blots. The combined data from three experiments did not reveal significant difference among parental, GFP-transfected or claudin-7-GFP-transfected cells.

The decrease or increase of TER in claudin-7-overexpressing cells depended on the ionic compositions

The expression of claudin-7-GFP did not disrupt the tight junction barrier function, instead, the TER in *claudin-7*-transfected cells increased 100% compared to that of control cells when measured in the culture medium (Fig. 4A). Since the major ions conducting the current in the culture medium were Na^+ and Cl^- , we then measured the TER in a defined solution containing 140 mM NaCl (P1 buffer). Similarly, the

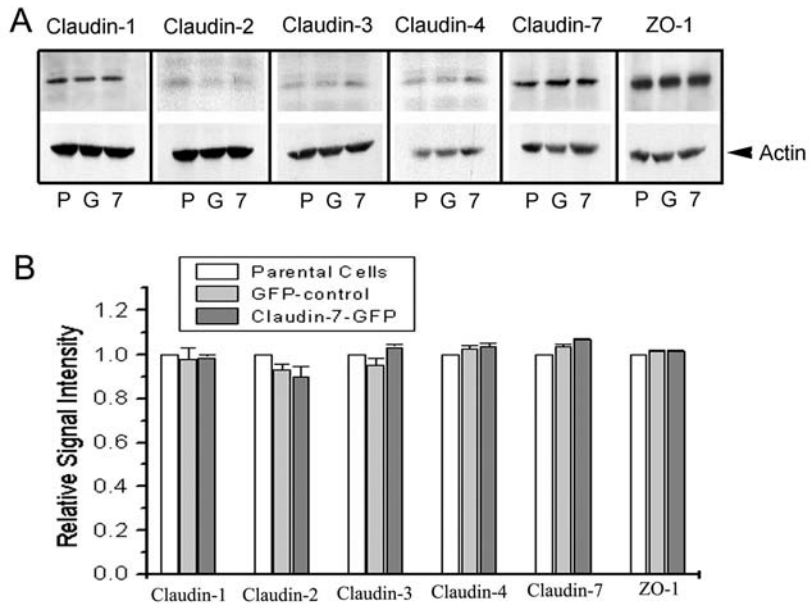
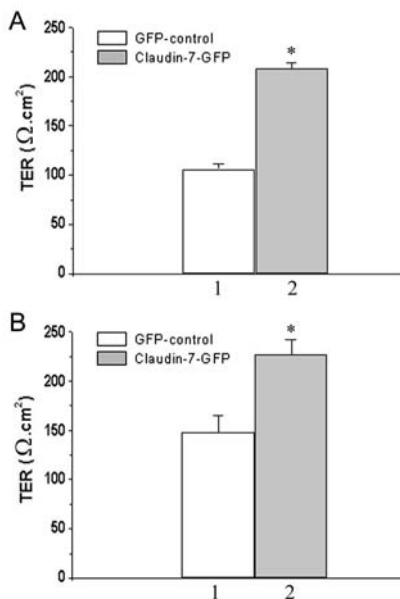


Fig. 3. Immunoblot analysis of endogenous tight junction proteins in parental, GFP-transfected, and *claudin-7*-GFP-transfected cells (mixed clones). (A) Parental (P), GFP-transfected (G), and *claudin-7*-GFP-transfected (7) cells were lysed in RIPA buffer, and a total of 20 μ g protein for each lane was loaded onto the SDS-polyacrylamide gel. Membranes were blotted against claudin-1, -2, -3, -4, -7 and ZO-1 antibodies. Actin staining was used as a loading control. (B) Densitometry analysis of protein expression levels. Following immunoblotting, X-ray films were scanned and band images were analyzed. The relative signal intensity of each band was obtained after background subtraction. The band intensity for parental cells was normalized to 1 and set as the reference. Data were collected from three independent clones with high expression levels of GFP and *claudin-7*-GFP. The average density values for three separate experiments were plotted for each designated claudin protein.

TER in *claudin-7*-overexpressing cells was significantly higher (56% increase) than that of control cells when measured in P1 buffer (Fig. 4B).



The increase in TER measured in the culture medium or P1 buffer containing NaCl could reflect a decrease in Na^+ or Cl^- conductance (or both) in *claudin-7*-overexpressing cells. In order to distinguish between these possibilities, we replaced NaCl in P1 buffer with arginine-HCl or lysine-HCl to differentiate the charge selectivity of Cl^- from Na^+ in *claudin-7*-overexpressing cells. Arginine and lysine are chosen because they are organic molecules and positively charged in the solution at the neutral pH that can be used to replace Na^+ . In the presence of Cl^- ions without Na^+ ions, the TER was dramatically increased in the cells transfected with *claudin-7*-GFP compared to that of controls (Fig. 5A,B). This TER increase was more than that when using NaCl. Replacing Na^+ with arginine $^+$ or lysine $^+$ increased the TER by 170% and 160%, respectively, in *claudin-7*-overexpressing cells (Fig. 5A,B). This demonstrates that overexpression of *claudin-7* reduced the paracellular conductance to Cl^- ions.

The differences in TER measured in NaCl and arginine-HCl (or lysine-HCl) may reflect the greater permeability to Na^+ ions of the cells overexpressing *claudin-7*. To address this possibility, we replaced NaCl with sodium aspartate to examine the Na^+ effect. In the presence of sodium aspartate, the overall TER in both control and *claudin-7*-overexpressing cells were greatly increased. This is because LLC-PK1 cells are anion-selective and are less permeable to cations. Nevertheless, compared to the TER obtained from control cells, the TER in *claudin-7*-overexpressing cells was decreased 56% (Fig. 5C). This clearly suggests that overexpression of *claudin-7* not only decreased the paracellular conductance to Cl^- but also increased paracellular conductance to Na^+ . Since the overall TER was increased in the presence of NaCl, the decrease in the paracellular Cl^- conductance must be greater than the increase in the paracellular Na^+ conductance.

Overexpression of *claudin-7* resulted in an increased TER in the paracellular Cl^- permeability and an increase in the paracellular Na^+ permeability

To further examine the paracellular charge selectivity and confirm the results obtained from the TER measurements, we

Fig. 4. *Claudin-7* overexpression resulted in an increased TER in culture medium and P1 buffer. (A) LLC-PK1 cells were plated on Transwell plates and cultured for 7 days. TER was measured in the culture medium and determined as described in Materials and Methods. *Claudin-7*-overexpressing cells (2) showed significantly higher TER ($P < 0.001$) than that of control cells (1). (B) TER was measured in P1 buffer containing 140 mM NaCl. Cells overexpressing *claudin-7* (2) had a significant increase ($P < 0.01$) in TER compared to that of control cells (1). Data are represented as means \pm s.e.m. from at least three mixed clones with 24 monolayers ($n = 24$) for each experiment. Student's *t*-test was used for statistical analysis.

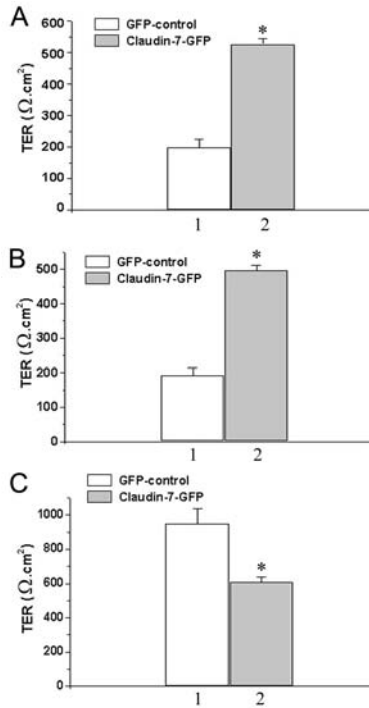


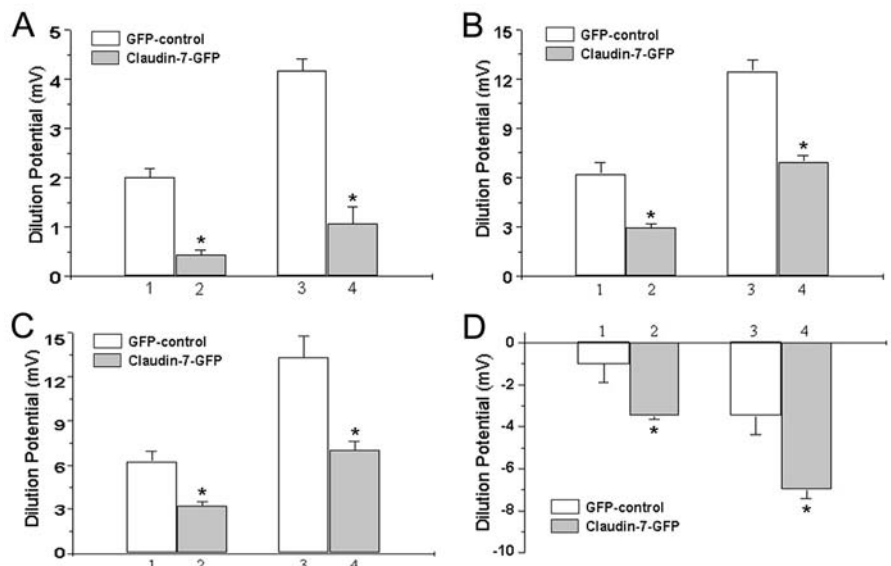
Fig. 5. Effect of claudin-7 overexpression on TER in modified P1 buffer. (A) TER measurements were performed on LLC-PK1 cells grown on Transwell plates. 140 mM NaCl in P1 buffer was replaced by 140 mM arginine-HCl. In the solution, HCl dissociated into H^+ and Cl^- , and H^+ bound to OH^- in the solution to form water at pH 7.3. Without Na^+ in the solution, TER was dramatically increased in cells overexpressing claudin-7 (2) compared to that of control cells ($P < 0.001$). (B) The experimental condition was similar to that in A, but 140 mM NaCl was substituted by 140 mM lysine-HCl. A significant increase in TER was also observed in cells overexpressing claudin-7 (2) ($P < 0.001$). (C) In contrast, TER significantly decreased ($P < 0.01$) in claudin-7-overexpressing cells when 140 mM NaCl was replaced with 140 mM sodium aspartate (2). Data were obtained from at least three mixed clones ($n = 24$ for each experiment) and presented as means \pm s.e.m.

performed electrophysiological experiments to measure the transepithelial dilution potentials in claudin-7-transfected cells and control cells. In mock-transfected cells, the dilution potential was positive when the concentration of NaCl in the apical chamber was kept constant at 140 mM (P1), but its concentration in the basal chamber was changed from 140 mM to either 70 mM (P2) or to 35 mM (P3) (Fig. 6A, column 1

and 3). This result confirms that LLC-PK1 cells are anion-selective and more permeable to anions than cations, which is consistent with previous reports (Van Itallie et al., 2003). However, under the same condition, the dilution potential was dramatically reduced (350% decrease in P2 and 300% decrease in P3) in the cells overexpressing claudin-7 (Fig. 6A, column 2 and 4). This could result from a decrease in the paracellular permeability to Cl^- or an increase in the paracellular permeability to Na^+ or both.

To determine the contribution of Cl^- and Na^+ in the paracellular charge selectivity on claudin-7-overexpressing cells, NaCl was replaced by arginine-HCl, lysine-HCl, or sodium aspartate in all three buffers (P1, P2, and P3). As shown in Fig. 6B, when the buffer in the basal chamber was changed from 140 mM arginine-HCl to either 70 mM (Fig. 6B, column 1 and 2) or 35 mM arginine-HCl (Fig. 6B, column 3 and 4), the dilution potentials in claudin-7-overexpressing cells were

Fig. 6. Dilution potential measurements revealed that overexpression of claudin-7 decreased paracellular permeability to Cl^- and increased paracellular permeability to Na^+ . (A) LLC-PK1 cells stably transfected with GFP or *claudin-7*-GFP were grown on Snapwell filters. Once monolayers reached confluence, the filter rings containing cell monolayers were mounted into EasyMount chambers. Both apical and basal chambers were filled with P1 buffer containing 140 mM NaCl. Subsequently, P1 buffer in the basal chamber was replaced by P2 buffer with 70 mM NaCl (1 and 2) or P3 buffer with 35 mM NaCl (3 and 4). Dilution potential values were significantly lower ($P < 0.001$) in claudin-7-overexpressing cells (2 and 4) compared to that of controls (1 and 3). The reduction in dilution potentials was a combined effect of Na^+ and Cl^- . (B) The experimental procedure was the same as in A except that NaCl in P1, P2 and P3 buffers was replaced by arginine-HCl to remove the contribution of Na^+ on the reduction of dilution potentials in cells overexpressing claudin-7. In this case, dilution potential values were reduced 100% ($P < 0.001$) in claudin-7-overexpressing cells (2 and 4) compared to that of controls (1 and 3). (C) NaCl was replaced by lysine-HCl in the P1, P2 and P3 buffers. The percentage decrease in dilution potentials was almost the same as with arginine-HCl ($P < 0.001$). (D) To eliminate the contribution of Cl^- to the dilution potential, sodium aspartate was used in all three buffers. In the absence of a Cl^- concentration gradient, the dilution potentials in both control and claudin-7-overexpressing cells changed from positive to negative. The dilution potentials did not decrease; instead, they significantly increased ($P < 0.001$) in cells overexpressing claudin-7 (2 and 4) compared to controls (1 and 3). Data are represented as means \pm s.e.m. from at least three mixed clones ($n = 12$ for each experiment).



reduced 100% compared to those of the control cells in both cases. Similar results were obtained when using lysine-HCl (Fig. 6C). Therefore, it is clear that in the absence of Na^+ , dilution potentials were decreased in the cells overexpressing claudin-7, although the reduction magnitude was not as great as those measured in NaCl solution (Fig. 6A). This indicated that Na^+ also contributed to the decrease in dilution potentials seen in Fig. 6A. Indeed, when substituting NaCl with sodium aspartate in P1, P2 and P3 buffers, the dilution potentials reversed their direction and changed from positive to negative, indicating the change of the monolayers from anion-selective to cation-selective (Fig. 6D). More strikingly, in the absence of the Cl^- concentration gradient, the dilution potentials in claudin-7-overexpressing cells were increased 250% in P2 (Fig. 6D column 2) and 100% in P3 (Fig. 6D column 4) compared to those of control cells, suggesting that they were more permeable to Na^+ than the control cells. All these results confirmed the data obtained from the TER measurements that overexpression of claudin-7 reduced the paracellular conductance to Cl^- while it increased the paracellular conductance to Na^+ .

We have also transfected *claudin-7*-GFP into MDCK II cells. Although TER was slightly increased, we did not observe

any difference in dilution potentials in MDCK II cells overexpressing claudin-7 compared to that of mock-transfected cells (data not shown).

Changes in TER and dilution potentials were associated with the expression level of claudin-7-GFP

To investigate whether the change in the ion selectivity observed in *claudin-7*-GFP-transfected cells was related to claudin-7, we selected individual clones with low, medium, or high expression levels of claudin-7-GFP (Fig. 7A) to measure their TER and dilution potentials. The TER values were well correlated with the expression level of claudin-7-GFP as shown by Fig. 7B. The higher the expression level of claudin-7-GFP, the greater the TER increased when compared to that of GFP-transfected cells. This correlation was also observed when dilution potentials were measured using buffer containing lysine-HCl or sodium aspartate.

When the lysine-HCl concentration was changed from 140 mM to 70 mM in the basal chamber, the dilution potentials in claudin-7-overexpressing cells were reduced with the increasing level of claudin-7-GFP expression compared to that of control cells (Fig. 7C, column 1: GFP; column 2: low; column 3: medium; column 4: high). Similar results were obtained when the lysine-HCl concentration in the basal chamber was changed from 140 mM to 35 mM (Fig. 7C, column 5, GFP; column 6, Low; column 7, Medium; column 8, High). These data indicated that the higher the expression level of claudin-7, the less Cl^- could pass through the monolayer, which resulted in the reduced dilution potential.

In contrast, when sodium aspartate concentration in the basal chamber was changed from 140 mM to 70 mM (Fig. 7D,

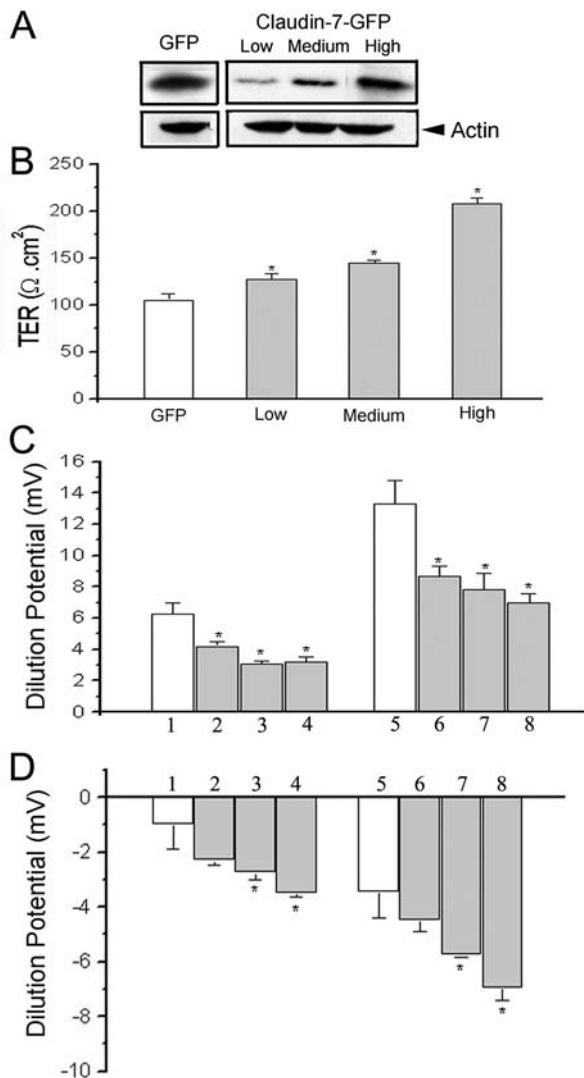


Fig. 7. The correlation between claudin-7-GFP expression levels and changes in TER and dilution potentials. (A) Immunoblot analysis of claudin-7-GFP expression level. Three single clones were selected for each expression group. Lysates with equal total protein concentration were obtained from cells expressing low, medium and high levels of claudin-7-GFP protein. Immunoblots were probed with anti-GFP polyclonal antibody to detect claudin-7-GFP fusion protein (49 kDa) and GFP (27 kDa). Anti-actin staining was used as a loading control. (B) TER was measured, in the culture medium, on triplicate filters of three different clones expressing low, medium and high levels of claudin-7-GFP protein. A dose response increase in TER was correlated with the increasing expression level of claudin-7-GFP. (C) Dilution potential measurements were performed to determine the relationship between the ion selective and claudin-7-GFP expression level. Cells were grown on Snapwell filters for 8 days. Triplicate filters were used for measurement of dilution potentials in modified P buffer containing 140 mM lysine-HCl. When lysine-HCl concentration in the basal chamber was changed from 140 mM to 70 mM (column 1-4) or to 35 mM (column 5-8) while keeping the apical chamber constant at 140 mM, cells expressing low (column 2 and 6), medium (column 3 and 7) and high (column 4 and 8) levels of claudin-7-GFP displayed a progressive decrease in dilution potentials compared to that of control cells (column 1 and 5). (D) The experimental procedure was the same as described in C except that dilution potentials were measured in buffer containing sodium aspartate. Results indicated a dose response increase in dilution potentials from cells expressing increased levels of claudin-7-GFP (low: column 2 and 6; medium: column 3 and 7; high: column 4 and 8) compared to that of controls (column 1 and 5). *The value is significantly different from the control ($P < 0.05$).

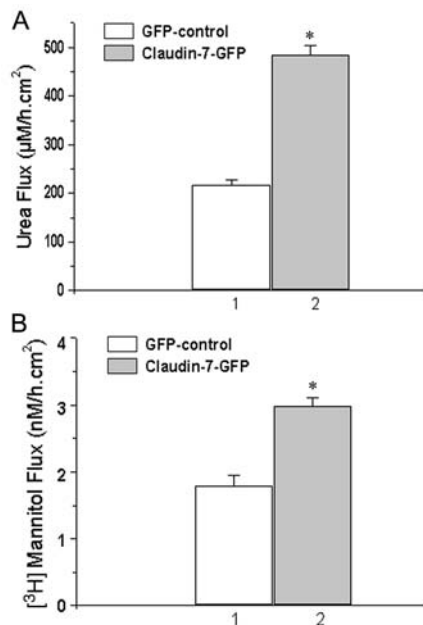


Fig. 8. Paracellular flux of neutral molecules. (A) Paracellular urea flux. Cells were grown on Transwell membranes until confluent. 50 mM urea was added to the basal solution. After incubation for 1 hour at 37°C, 300 µl aliquot was removed from the apical solution. Urea concentration was measured by an ACE clinical chemistry analyzer. Data are represented as means \pm s.e.m. from three independent clones ($n=12$ for each experiment). Urea flux in claudin-7-overexpressing cells (2) was 120% higher ($P<0.001$) compared to that of the control cells (1). TER was measured in growth media before and after each paracellular urea flux experiment to confirm that the monolayer remained intact during the flux experiments. (B) Mannitol flux. Control or claudin-7-overexpressing cells were plated on Transwell plates until confluent. The basal culture medium was supplemented with 1 mM cold mannitol. The apical medium was the same as the basal medium except that it contained 1 µCi/ml [^3H]mannitol. After 1 hour incubation at 37°C, 100 µl of basal medium were taken and replaced with 100 µl fresh medium containing 1 mM unlabeled mannitol. The radioactivity of the 100 µl samples was measured. Data are means \pm s.e.m. from three independent clones ($n=12$ for each experiment). Mannitol flux in claudin-7-overexpressing cells (2) was significantly higher ($P<0.001$) compared to controls (1).

columns 1-4) or to 35 mM (Fig. 7D, columns 5-8), the dilution potentials were steadily increased with the increasing level of claudin-7-GFP expression. These results suggested that cells with higher levels of claudin-7 expression were more permeable to Na^+ than that of control cells and cells with lower levels of claudin-7-GFP expression. The outcome of these experiments did not change with or without geneticin in the solution (data not shown).

Overexpression of claudin-7 increased the paracellular flux to uncharged solutes

We next asked whether overexpression of claudin-7 would affect the paracellular flux to neutral molecules. Urea and mannitol were used to perform these experiments since these two neutral molecules were often selected in tracer flux study (McCarthy et al., 2000; Tang and Goodenough, 2003; Yu et al.,

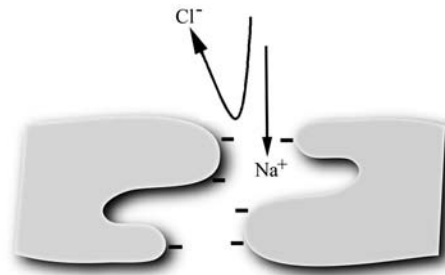


Fig. 9. A model of the paracellular channel formed by claudin-7. The extracellular domains of claudin-7 from opposing cells constitute a paracellular channel. The mouth of the channel from both sides is negatively charged, which hinders Cl^- entry while allowing Na^+ to go through.

2003). Both control and claudin-7-overexpressing cells were plated on the Transwell membrane until confluent. Urea (M_r 60) was applied to the basal solution, and samples were taken from the apical solution after incubation for 1 hour at 37°C. It is clear from Fig. 8A that the urea flux was increased 125% on cells overexpressing claudin-7 compared to that of control cells. The paracellular mannitol (M_r 182) flux was increased 70% in cells transfected with *claudin-7-GFP* compared to the controls (Fig. 8B). These results indicated that overexpression of claudin-7 not only influenced the charge selectivity of the cell monolayers but also the paracellular flux to neutral molecules.

Discussion

Claudins play a vital role in various physiological functions in vivo, including Mg^{2+} resorption in the renal tubule, formation of the epidermal water barrier and the blood brain barrier, sperm maturation, and fluid compartmentalization in the inner ear (Gow et al., 1999; Simon et al., 1999; Turksen and Troy, 2001; Wilcox et al., 2001; Furuse et al., 2002; Ben-Yosef et al., 2003; Nitta et al., 2003; Gow et al., 2004). Several reports indicated that claudins exert their function by forming ion-selective paracellular channels or by creating paracellular ion-selective permeability barriers (Amasheh et al., 2002; Colegio et al., 2002; Yu et al., 2003). In this study, we have shown, for the first time, that overexpression of claudin-7 resulted in a decrease in the paracellular conductance to Cl^- as well as a concurrent increase in the paracellular conductance to Na^+ in LLC-PK1 cells. Expression of claudin-7-GFP neither affected the localization of endogenous tight junction proteins nor disrupted the tight junction barrier function. TER was greatly increased in claudin-7-overexpressing cells when measured in the culture medium or in the solutions containing Cl^- but was significantly decreased when replacing NaCl with sodium aspartate in the solution. Results obtained from dilution potentials also demonstrated that claudin-7-overexpressing cells were less permeable to Cl^- but more permeable to Na^+ compared to those of mock-transfected cells. These ion selective properties were well correlated with the expression level of claudin-7-GFP.

We have compared the expression levels of endogenous claudin-1, -2, -3, -4, -7, and ZO-1 in parental, GFP-transfected and *claudin-7-GFP*-transfected LLC-PK1 cells from three high

expression clones (Fig. 3). Although claudin-2 expression level was somewhat decreased in both GFP- and *claudin-7*-GFP-transfected cells compared to that of parental cells, this decrease is unlikely to affect our conclusion that claudin-7 overexpression decreases paracellular conductance to Cl^- since we are comparing data between GFP- and *claudin-7*-GFP-transfected cells. In addition, the primary localization site of claudin-2 was not at the cell-cell junction. Claudin-3 and -4 were slightly increased in *claudin-7*-GFP-transfected cells compared to that of GFP-transfected and parental cells. Overexpression of claudin-4 has been reported to reduce the paracellular permeability specific to Na^+ , which is opposite to what we have seen for the effect of claudin-7 overexpression. It is possible, but less likely, that the slightly increased claudin-3 expression level caused the ion selectivity we have seen in claudin-7-overexpressing cells. Overexpression of claudin-3 in epithelial cells has been reported to decrease the solute permeability but it did not increase TER significantly compared to that of control cells (Coyne et al., 2003). Moreover, we observed a close correlation between claudin-7 overexpression and changes in TER and dilution potentials (Fig. 7).

Ion substitution is a commonly used method to study channel properties in the field of ion channel research (Keramidas et al., 2002; Hansen et al., 2004; Lai et al., 2004). For example, aspartate (Asp^-) and glutamate (Glu^-) have been used to replace Cl^- to study the transient outward K channel in rat ventricular myocytes (Lai et al., 2004). NH_4Cl , TriMAHCl (trimethylammonium hydrochloride), Tris-HCl (Tris[hydroxymethyl]aminomethane hydrochloride), and TEACl (tetraethylammonium chloride) have been used to replace Na^+ in the solution to study the glycine receptor channel in HEK293 cells (Keramidas et al., 2002). In this study, we also used the ion substitution method to differentiate the effect of Cl^- from Na^+ on claudin-7-overexpressing cells. We choose arginine, lysine and aspartate to substitute for Na^+ and Cl^- because they are not neural transmitters and do not have biochemically active groups on the molecules to interact with cell membrane components. Although it was unclear whether arginine⁺ and lysine⁺ went through the paracellular route in LLC-PK1 cells, the TER values were much higher when using Arg^+ and Lys^+ than when using Na^+ (as shown in Figs 4 and 5), which suggested that they were less permeable than Na^+ . The change of dilution potential from positive to negative (Fig. 6D and Fig. 7D) indicated that aspartate⁻ was relatively impermeable to the paracellular pathway in LLC-PK1 cells.

Overexpression of a claudin in epithelial cells could either increase or decrease TER or could change the paracellular permeability for a particular ion (Inai et al., 1999; McCarthy et al., 2000; Furuse et al., 2001; Van Itallie et al., 2003). Our study shows that overexpression of one claudin could result in a decreased paracellular permeability to one type of ion and an increased paracellular permeability to another type of ion. One model to explain this result is that claudin-7 forms a paracellular channel with negative charges on the entry wall of the channel (Fig. 9). This would prevent negative ions from entering the pore while allowing positive ions to pass through the channel. Another possibility is that claudin-7 forms a paracellular barrier to Cl^- . However, overexpression of claudin-7 affects other paracellular channels that could increase the

paracellular permeability to Na^+ . It is reasonable to postulate that the paracellular channel formed by claudin-7 must have a stronger effect on hindering Cl^- permeation than on permitting Na^+ permeation since the TER measured in culture medium or in the solution containing NaCl was significantly increased in claudin-7-overexpressing cells compared to controls.

We observed that the overexpression of claudin-7-GFP in MDCK II cells resulted in no difference in dilution potentials compared to that of mock-transfected cells (data not shown). This suggested that the cellular background is important in determining the electrophysiological property of a claudin. LLC-PK1 cells are more permeable to anions than cations, whereas the function of claudin-7 may be to form a paracellular permeability barrier to Cl^- . Because the charge selectivity of claudin-7 was the opposite to that of LLC-PK1 cells, it can be detected more easily in this cell line than in the MDCK II cell line. Van Itallie et al. reported similar observation in their studies (Van Itallie et al., 2003). Claudin-8 has been suggested to form the paracellular barrier to Na^+ permeation when expressed in MDCK II cells (Yu et al., 2003). Since claudin-7 and -8 are both localized at the distal nephron, they must interact with each other in vivo to regulate the overall paracellular permeability to Na^+ and Cl^- under the normal physiological condition.

Overexpression of claudin-7 not only affected the charge selectivity of LLC-PK1 cells but also the paracellular flux of neutral molecules. At the present time, it is unclear whether the increase in urea and mannitol paracellular flux is directly related to claudin-7 function or is caused by the secondary effect of claudin-7 overexpression. For example, the overexpression of claudin-7 may lead to an increase in pore size or the number of paracellular channels permeable to the neutral molecules. The increases in both TER and paracellular flux to neutral molecules have been reported by Balda et al. (Balda et al., 1996). It is possible that ion conductance and solute flux are two separable events as recently proposed by Anderson et al. (Anderson et al., 2004). More studies are needed to address the question of whether the paracellular ion transport and uncharged solute transport are regulated through two different mechanisms.

If the function of claudin-7 in vivo is to form a paracellular permeability barrier to Cl^- , mutations in the claudin-7 gene may cause the backleak of Cl^- in the distal nephron and, therefore, increase the Na^+ resorption, which could lead to hypertension in affected individuals. The challenge we have now is to determine how these paracellular channels work and what are the underlying mechanisms controlling claudin assembly, interactions and regulations.

We thank Mark Knepper (NIH) for providing the TSC and BSC-1 antibodies. We also thank Ruth Schwalbe for helpful suggestion and discussions and Donald Fletcher for reading the manuscript. We acknowledge Beverly Jeansonne, George W. Lanford and Joan T. Zary for their technical assistance. This work was supported by an ECU Faculty Research Award to Y.H.C. and an American Cancer Society Research Award to Q.L.

References

- Alexandre, M. D. and Chen, Y. H. (2003). Claudin-7 overexpression decreases the paracellular conductance in kidney epithelial cells. *Mol. Biol. Cell* **14**, 459a.

- Amasheh, S., Meiri, N., Gitter, A. H., Schoneberg, T., Mankertz, J., Schulzke, J. D. and Fromm, M. (2002). Claudin-2 expression induces cation-selective channels in tight junctions of epithelial cells. *J. Cell Sci.* **115**, 4969-4976.
- Anderson, J. M., Van Itallie, C. M. and Fanning, A. S. (2004). Setting up a selective barrier at the apical junction complex. *Curr. Opin. Cell Biol.* **16**, 140-145.
- Balda, M. S., Whitney, J. A., Flores, C., Gonzalez, S., Cerejido, M. and Matter, K. (1996). Functional dissociation of paracellular permeability and transepithelial electrical resistance and disruption of the apical-basolateral intramembrane diffusion barrier by expression of a mutant tight junction membrane protein. *J. Cell Biol.* **134**, 1031-1049.
- Ben-Yosef, T., Belyantseva, I. A., Saunders, T. L., Hughes, E. D., Kawamoto, K., Van Itallie, C. M., Beyer, L. A., Halsey, K., Gardner, D. J., Wilcox, E. R. et al. (2003). Claudin 14 knockout mice, a model for autosomal recessive deafness DFNB29, are deaf due to cochlear hair cell degeneration. *Hum. Mol. Genet.* **12**, 2049-2061.
- Chen, Y. H., Lu, Q., Goodenough, D. A. and Jeansonne, B. (2002). Nonreceptor tyrosine kinase c-Yes interacts with occludin during tight junction formation in canine kidney epithelial cells. *Mol. Biol. Cell* **13**, 1227-1237.
- Colegio, O. R., Van Itallie, C. M., McCrea, H. J., Rahner, C. and Anderson, J. M. (2002). Claudins create charge-selective channels in the paracellular pathway between epithelial cells. *Am. J. Physiol. Cell Physiol.* **283**, C142-C147.
- Colegio, O. R., Van Itallie, C., Rahner, C. and Anderson, J. M. (2003). Claudin extracellular domains determine paracellular charge selectivity and resistance but not tight junction fibril architecture. *Am. J. Physiol. Cell Physiol.* **284**, C1346-C1354.
- Coyne, C. B., Gambling, T. M., Boucher, R. C., Carson, J. L. and Johnson, L. G. (2003). Role of claudin interactions in airway tight junctional permeability. *Am. J. Physiol. Lung Cell Mol. Physiol.* **285**, L1166-L1178.
- Furuse, M., Fujita, K., Hiiiragi, T., Fujimoto, K. and Tsukita, S. (1998). Claudin-1 and -2: novel integral membrane proteins localizing at tight junctions with no sequence similarity to occludin. *J. Cell Biol.* **141**, 1539-1550.
- Furuse, M., Furuse, K., Sasaki, H. and Tsukita, S. (2001). Conversion of zonulae occludentes from tight to leaky strand type by introducing claudin-2 into Madin-Darby canine kidney I cells. *J. Cell Biol.* **153**, 263-272.
- Furuse, M., Hata, M., Furuse, K., Yoshida, Y., Haratake, A., Sugitani, Y., Noda, T., Kubo, A. and Tsukita, S. (2002). Claudin-based tight junctions are crucial for the mammalian epidermal barrier: a lesson from claudin-1-deficient mice. *J. Cell Biol.* **156**, 1099-1111.
- Gonzalez-Mariscal, L., Betanzos, A., Nava, P. and Jaramillo, B. E. (2003). Tight junction proteins. *Prog. Biophys. Mol. Biol.* **81**, 1-44.
- Gow, A., Southwood, C. M., Li, J. S., Pariali, M., Riordan, G. P., Brodie, S. E., Danias, J., Bronstein, J. M., Kachar, B. and Lazzarini, R. A. (1999). CNS myelin and sertoli cell tight junction strands are absent in Osp/claudin-11 null mice. *Cell* **99**, 649-659.
- Gow, A., Davies, C., Southwood, C. M., Frolenkov, G., Chrustowski, M., Ng, L., Yamauchi, D., Marcus, D. C. and Kachar, B. (2004). Deafness in Claudin 11-null mice reveals the critical contribution of basal cell tight junctions to stria vascularis function. *J. Neurosci.* **24**, 7051-7062.
- Hansen, L. A., Dacheux, F., Man, S. Y., Clulow, J. and Jones, R. C. (2004). Fluid reabsorption by the ductuli efferentes testis of the rat is dependent on both sodium and chloride. *Biol. Reprod.* **71**, 410-416.
- Heiskala, M., Peterson, P. A. and Yang, Y. (2001). The roles of claudin superfamily proteins in paracellular transport. *Traffic* **2**, 93-98.
- Inai, T., Kobayashi, J. and Shibata, Y. (1999). Claudin-1 contributes to the epithelial barrier function in MDCK cells. *Eur. J. Cell Biol.* **78**, 849-855.
- Jeansonne, B., Lu, Q., Goodenough, D. A. and Chen, Y. H. (2003). Claudin-8 interacts with multi-PDZ domain protein 1 (MUPP1) and reduces paracellular conductance in epithelial cells. *Cell. Mol. Biol.* **49**, 13-21.
- Keramidas, A., Moorhouse, A. J., Pierce, K. D., Schofield, P. R. and Barry, P. H. (2002). Cation-selective mutations in the M2 domain of the inhibitory glycine receptor channel reveal determinants of ion-charge selectivity. *J. Gen. Physiol.* **119**, 393-410.
- Kiuchi-Saishin, Y., Gotoh, S., Furuse, M., Takasuga, A., Tano, Y. and Tsukita, S. (2002). Differential expression patterns of claudins, tight junction membrane proteins, in mouse nephron segments. *J. Am. Soc. Nephrol.* **13**, 875-886.
- Lai, X. G., Yang, J., Zhou, S. S., Zhu, J., Li, G. R. and Wong, T. M. (2004). Involvement of anion channel(s) in the modulation of the transient outward K(+) channel in rat ventricular myocytes. *Am. J. Physiol. Cell Physiol.* **287**, C163-C170.
- Li, W. Y., Huey, C. L. and Yu, A. S. (2004). Expression of claudin-7 and -8 along the mouse nephron. *Am. J. Physiol. Renal Physiol.* **286**, F1063-F1071.
- McCarthy, K. M., Francis, S. A., McCormack, J. M., Lai, J., Rogers, R. A., Skare, I. B., Lynch, R. D. and Schneeberger, E. E. (2000). Inducible expression of claudin-1-myc but not occludin-VSV-G results in aberrant tight junction strand formation in MDCK cells. *J. Cell Sci.* **113**, 3387-3398.
- Mitic, L. L., Van Itallie, C. M. and Anderson, J. M. (2000). Molecular physiology and pathophysiology of tight junctions I. Tight junction structure and function: lessons from mutant animals and proteins. *Am. J. Physiol. Gastrointest. Liver Physiol.* **279**, G250-G254.
- Morita, K., Furuse, M., Fujimoto, K. and Tsukita, S. (1999). Claudin multigene family encoding four-transmembrane domain protein components of tight junction strands. *Proc. Natl. Acad. Sci. USA* **96**, 511-516.
- Nitta, T., Hata, M., Gotoh, S., Seo, Y., Sasaki, H., Hashimoto, N., Furuse, M. and Tsukita, S. (2003). Size-selective loosening of the blood-brain barrier in claudin-5-deficient mice. *J. Cell Biol.* **161**, 653-660.
- Reyes, J. L., Lamas, M., Martin, D., del Carmen Namorado, M., Islas, S., Luna, J., Tauc, M. and Gonzalez-Mariscal, L. (2002). The renal segmental distribution of claudins changes with development. *Kidney Int.* **62**, 476-487.
- Schneeberger, E. E. and Lynch, R. D. (2004). The tight junction: a multifunctional complex. *Am. J. Physiol. Cell Physiol.* **286**, C1213-C1228.
- Simon, D. B., Lu, Y., Choate, K. A., Velazquez, H., Al-Sabban, E., Praga, M., Casari, G., Bettinelli, A., Colussi, G., Rodriguez-Soriano, J. et al. (1999). Paracellin-1, a renal tight junction protein required for paracellular Mg²⁺ resorption. *Science* **285**, 103-106.
- Tang, V. W. and Goodenough, D. A. (2003). Paracellular ion channel at the tight junction. *Biophys. J.* **84**, 1660-1673.
- Tsukita, S. and Furuse, M. (2000). The structure and function of claudins, cell adhesion molecules at tight junctions. *Ann. New York Acad. Sci.* **915**, 129-135.
- Turksen, K. and Troy, T. C. (2001). Claudin-6: a novel tight junction molecule is developmentally regulated in mouse embryonic epithelium. *Dev. Dyn.* **222**, 292-300.
- Turksen, K. and Troy, T. C. (2002). Permeability barrier dysfunction in transgenic mice overexpressing claudin 6. *Development* **129**, 1775-1784.
- Van Itallie, C., Rahner, C. and Anderson, J. M. (2001). Regulated expression of claudin-4 decreases paracellular conductance through a selective decrease in sodium permeability. *J. Clin. Invest.* **107**, 1319-1327.
- Van Itallie, C. M., Fanning, A. S. and Anderson, J. M. (2003). Reversal of charge selectivity in cation or anion-selective epithelial lines by expression of different claudins. *Am. J. Physiol. Renal Physiol.* **285**, F1078-F1084.
- Wilcox, E. R., Burton, Q. L., Naz, S., Riazuddin, S., Smith, T. N., Ploplis, B., Belyantseva, I., Ben-Yosef, T., Liburd, N. A., Morell, R. J. et al. (2001). Mutations in the gene encoding tight junction claudin-14 cause autosomal recessive deafness DFNB29. *Cell* **104**, 165-172.
- Wong, V. and Goodenough, D. A. (1999). Paracellular channels! *Science* **285**, 62.
- Yu, A. S., Enck, A. H., Lencer, W. I. and Schneeberger, E. E. (2003). Claudin-8 expression in Madin-Darby canine kidney cells augments the paracellular barrier to cation permeation. *J. Biol. Chem.* **278**, 17350-17359.